Korean J. Chem. Eng., **21**(2), 511-520 (2004)

Mass Transfer Studies on Ternary Systems in a Bench-scale Liquid-Liquid Extraction (LLX) Column and a Comparison with Simulations

Debjit Sanpui, Manish K. Singh and Ashok Khanna†

Department of Chemical Engineering, Indian Institute of Technology Kanpur, Kanpur-208 016 (U.P.) India
(*Received 17 April 2003 • accepted 10 October 2003*)

Abstract–Mass transfer studies in a laboratory scale extraction column have been conducted for Toluene-Acetone-Water and MIBK-Acetic Acid-Water systems. From these experiments stage-wise solute (Acetone or Acetic-Acid) composition profiles have been obtained for both dispersed and continuous phase. These composition profiles have been compared with those obtained from ASPENPLUS, CHEMSEP and LLXSIM simulators. For liquid-liquid equilibrium calculations all these simulators use UNIFAC and UNIQUAC model. The binary interaction parameters for the UNIFAC are inbuilt in ASPENPLUS and CHEMSEP. UNIQUAC binary parameters were borrowed from DECHEMA. Error square analysis indicates that simulations based on *non-equilibrium* option of LLXSIM match *closely* with experimental results. Temperature profiles and hydrodynamic features characterized by number of drops and static holdup on the stages have been compared between the LLXSIM simulated and the experimental results and these match well. However simulations on ASPENPLUS give sum of relative error-squares for all the experimental runs at least *ten times higher*, in spite of tuning the average stage efficiency.

Key words: Liquid-liquid Extraction, Non-isothermal, Non-equilibrium, UNIFAC/UNIQUAC, Ternary Systems

INTRODUCTION

Liquid-liquid extraction is used for separating the components of a solution. All industrial applications are mostly non-isothermal operation and never reach equilibrium. Several commercial software packages such as ASPENPLUS (based on equilibrium model) and CHEMSEP (both the equilibrium and non-equilibrium models) are available to simulate the liquid-liquid extraction processes. In 1981 Kehat and Ghitis [Kehat and Ghitis, 1981] developed a computer program for the simulation of an extraction column. Using this simulation program they validated only the end point compositions in lab and industrial scale extraction columns. Zimmermann and co-workers [Zimmermann et al., 1995] have also shown comparison of stage-wise composition profiles for lab scale *Toluene-Acetone-Water* pulsed extraction column with their simulations based on isothermal rate based model. Chun and co-workers [Chun et al., 1996] have shown hydrodynamic validation in the spray column liquid-liquid extraction at supercritical condition. In this present work, two laboratory scale extraction operations with *Toluene-Acetone-Water* (TAW) and *Methyl-isobutyl-ketone* (MIBK)-*Acetic Acid-Water* (MAW) systems were compared with simulations using ASPENPLUS, CHEMSEP and our rate-based simulator - LLXSIM packages [Debjit and Khanna, 2000].

The aim of this work is to compare a laboratory scale liquid-liquid extraction operation with simulations based on the non-equilibrium approach. The essential features of a non-equilibrium model accounting both for heat and mass transfer are briefly presented in the Appendix.

EXPERIMENTS

†To whom correspondence should be addressed.
E-mail: akhanna@iitk.ac.in

Table 1. Column specification

Column specification:	
Column diameter	0.102 m
No. of stages	8
Sieve tray spacing	0.2 m
No. of holes (sieve)	120
Sieve hole diameter	0.00318 m
Feed location:	
Feed	@ 8 stage (bottom)
Solvent	@ 1 stage (top)

1. Bench Scale Extraction Column

The liquid-liquid extraction was studied in a 10.2 cm diameter and 1.78 m high glass column having eight aluminum sieve trays. A cylindrical down-comer made of aluminum was fixed in each tray. A spiral shaped distributor was used to disperse the light phase at the bottom of the column. To avoid corrosion, Stainless steel and Teflon pipelines were used. To draw the samples of both phases from each stage, sample ports (stopcock made of glass) were provided in the glass column. Details of the column and trays are given in Table 1 and the complete experimental setup is shown in Fig. 1. In this study, heavy continuous phase is fed from the top and the light dispersed phase is fed at the bottom of the column. At the start of the run, the column was filled with heavy continuous phase approximately up to the continuous phase inlet. Then light dispersed phase line was opened. The column was operated in both isothermal and non-isothermal conditions until steady state conditions were reached, which was indicated by constant height of coalesced layer on each tray.

2. Bench Scale Experiments

The ternary systems that were chosen for the comparison in the present work are TAW and MAW. In the TAW system, components

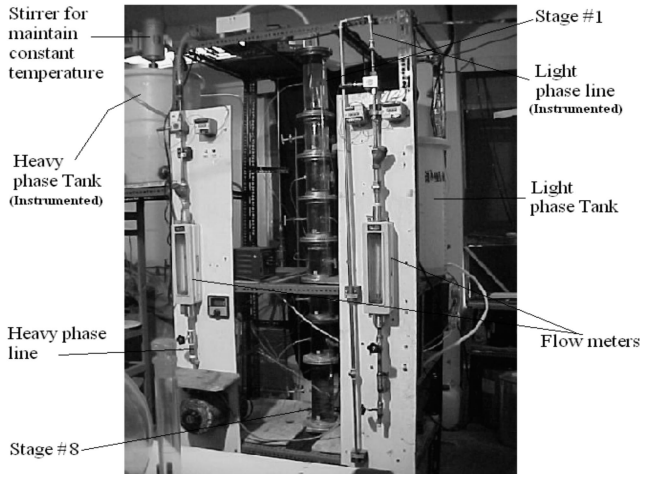

Fig. 1. Bench-scale liquid-liquid extraction column.

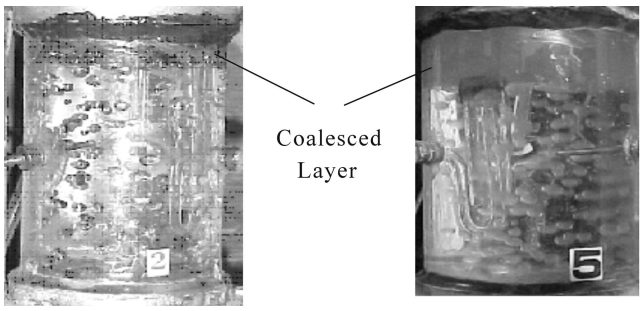

Fig. 2. Coalesced layer and light phase drops in stages.

can be easily separated with the help of conventional distillation procedure, but for the MAW system MIBK and Acetic Acid form an azeotrope and can only be separated by extraction. To observe the column performance and its comparison with the available simulators, seventeen bench scale runs with different solute concentrations and solvent to feed ratios (*S/F*) and different temperature drops (between top and bottom of the column) were done. The details of the individual runs are shown in Table 2.

3. Data Collection

3-1. Sample Collection from the Different Stages

The column was operated for 45 minutes for each run. Steady state for all the runs was attained approximately after 20 minutes. As mentioned earlier, to collect the samples for both the phases (heavy and light) glass stopcock arrangements were done in all eight stages. Samples from all the eight stages were collected and stored in air-tight sample bottles for component analysis.

3-2. Static Holdup and Number of Drops Measurements

The static holdups and the number of drops were measured on each stage for all the runs. At steady state, the static holdup stabilizes for all the stages. The holdup measurements were done with the help of a scale attached to the extraction column and with photography. The light-dispersed phase is fed from bottom of the extraction column and the dispersed light phase droplets travel upwards. The drops on each stage have been snapped with digital camera. The number of drops was counted after enlarging and scanning the digital photographs. One sample static holdups and drops of light phase are shown in Fig. 2.

3-3. Measurement of Light and Heavy Phase Temperatures

ASPENPLUS and CHEMSEP simulators give a stage temperature indicating that both phases leave the stage at the same temperature. But for non-isothermal liquid-liquid extraction, it is observed that

Table 2. Bench scale experiments with TAW and MAW systems

Run no.	*S/F* ratio	Feed* (mole %)	Feed temperature °C	Solvent temperature °C
Toluene-Acetone-Water system :: Solute : Acetone				
1	3	10% Acetone+90% Toluene	32.0	32.0
2	4	10% Acetone+90% Toluene	32.0	32.0
3	3	15% Acetone+85% Toluene	32.0	32.0
4	4	15% Acetone+85% Toluene	32.0	32.0
5	3	10% Acetone+90% Toluene	32.0	40.0
6	4	10% Acetone+90% Toluene	32.0	40.0
7	3	15% Acetone+85% Toluene	32.0	40.0
8	4	15% Acetone+85% Toluene	32.0	40.0
9	3	10% Acetone+90% Toluene	33.0	50.0
10	4	10% Acetone+90% Toluene	33.0	50.0
11	3	15% Acetone+85% Toluene	33.0	50.0
12	4	15% Acetone+85% Toluene	33.0	50.0
MIBK-Acetic Acid-Water system :: Solute : Acetic Acid				
13	3	9.3% Acetic Acid+2.2% Water+88.5% MIBK	30.0	30.0
14	3	9.25% Acetic Acid +2.05% Water+88.7% MIBK	30.0	45.0
15	2	9.25% Acetic Acid+2.05% Water+88.7% MIBK	30.0	45.0
16	2	7.15% Acetic Acid+2% Water+90.85% MIBK	33.5	50.0
17	3	7.15% Acetic Acid+2% Water+90.85% MIBK	33.5	50.0

*For all the runs Water is the solvent.

both liquids maintain their own distinct temperature profile throughout the column though they come in close contact with each other. Our rate-based simulator LLXSIM can calculate these phasic temperatures on each stage. To measure the heavy phase temperature, thermocouple probes have been inserted in each of the stages of our bench scale experimental column. For the light phase, the temperatures were measured at the time of sample collection. A highly sensitive thermometer in the range 0-100 °C was dipped in the sample bottle at the time of sample withdrawal for the light phases.

4. Composition Analysis

All the samples were analyzed on a Gas Chromatograph (GC) with Porapac-Q packed column (SS column, 1/8" OD, 1.5 meter length). The GC was operated in isothermal mode at 200 °C oven temperature and 210 °C thermal conductivity detector (TCD) tem-

Table 3. Binary interaction parameters for TAW and MAW systems [at 30 °C]

UNIQUAC Data (Macedo and Rasmussen [1987])**:**

Toluene(1)-Acetone(2)-Water(3) system				MIBK(1)-Acetic Acid(2)-Water(3)			
	1	2	3		1	2	3
R_k	3.923	2.574	0.920	R_k	4.596	2.203	0.920
Q_k	2.968	2.336	1.400	Q_k	3.592	2.072	1.400
1	0.000	269.90	987.42	1	0.000	−225.65	437.77
2	−138.80	0.000	390.94	2	−13.13	0.000	−278.08
3	172.79	−86.30	0.000	3	107.98	128.06	0.000

UNIFAC Data (Weidlich and Gmehling [1987])**:**

For TAW system

Components	UNIFAC groups
Toluene	5 ACH 1 $ACCH_3$
Acetone	1 CH_3 1 CH_3CO
Water	1 H_2O

	CH_3	ACH	$ACCH_3$	H_2O	CH_3CO
R_k	0.9	0.53	1.27	0.92	1.67
Q_k	0.85	0.4	0.97	1.4	1.49

Interaction terms

	CH_3	ACH	$ACCH_3$	H_2O	CH_3CO
CH_3	0	−114.8	−115.7	1300	472.6
ACH	156.5	0	167	859.4	593.7
$ACCH_3$	104.3	−146.8	0	5695	916.7
H_2O	342.4	372.8	203.7	0	−171.8
CH_3CO	66.56	−78.31	−73.87	634.8	0

For MAW system

Components	UNIFAC groups
MIBK	1 CH_2 2 CH_3 1 CH 1 CH_3CO
Acetic acid	1 CH_3 1 COOH
Water	1 H_2O

	CH_2	CH_3	CH	H_2O	CH_3CO	COOH
R_k	0.67	0.9	0.45	0.92	1.67	1.3
Q_k	0.54	0.85	0.23	1.4	1.49	1.22

Interaction terms

	CH_2	CH_3	CH	H_2O	CH_3CO	COOH
CH_2	0	0	0	1300	472.6	139.4
CH_3	0	0	0	1300	472.6	139.4
CH	0	0	0	1300	472.6	139.4
H_2O	342.4	342.4	342.4	0	−171.8	−465.7
CH_3CO	66.56	66.56	66.56	634.8	0	1247
COOH	1744	1744	1744	652.3	−101.3	0

perature. As an example for the TAW system, the GC was calibrated with different known concentrations of Toluene-Acetone along with a known amount of Water (0 to 5% in interval of 1%); and Acetone-Water along with a known amount of Toluene (0 to 5% in interval of 1%) mixtures. Mole fraction versus area curves for these known samples were prepared. Then each sample obtained from the different stages of the LLX column was analyzed at above the GC temperature setting. Though the diffusivity of light component Toluene/MIBK is much less in Water phase, one cannot neglect its presence. Similarly, the presence of water cannot be ignored in the light Toluene/MIBK phase. Compared with the calibrated mole fraction of pure component versus area plots, the concentration of solute was obtained for each sample for both the phases.

RESULTS AND DISCUSSION

The objective of this work was to compare the bench-scale liquid-liquid extraction runs with the available simulators. To compare the experimental results all the simulators (ASPENPLUS, CHEMSEP and LLXSIM) were run with the same column configuration and operating conditions as in the lab scale experiments. ASPENPLUS does not accept any column specifications, so only eight equilibrium stages were considered. As mentioned earlier, all the real liquid-liquid extraction processes never reach equilibrium; non-equilibrium features with respect to both the heat and mass transfer predominate. To consider these, a non-equilibrium model for CHEMSEP has been invoked. In the CHEMSEP simulator, there is only one mass transfer coefficient option for liquid-liquid extraction, i.e., the Handlos-Baron correlation [Handlos and Barron, 1957]. To calculate this binary mass transfer coefficient, diffusivity correlation [Wesselingh and Krishna, 1990] for concentrated mixtures and [Siddiqi and Lucas,

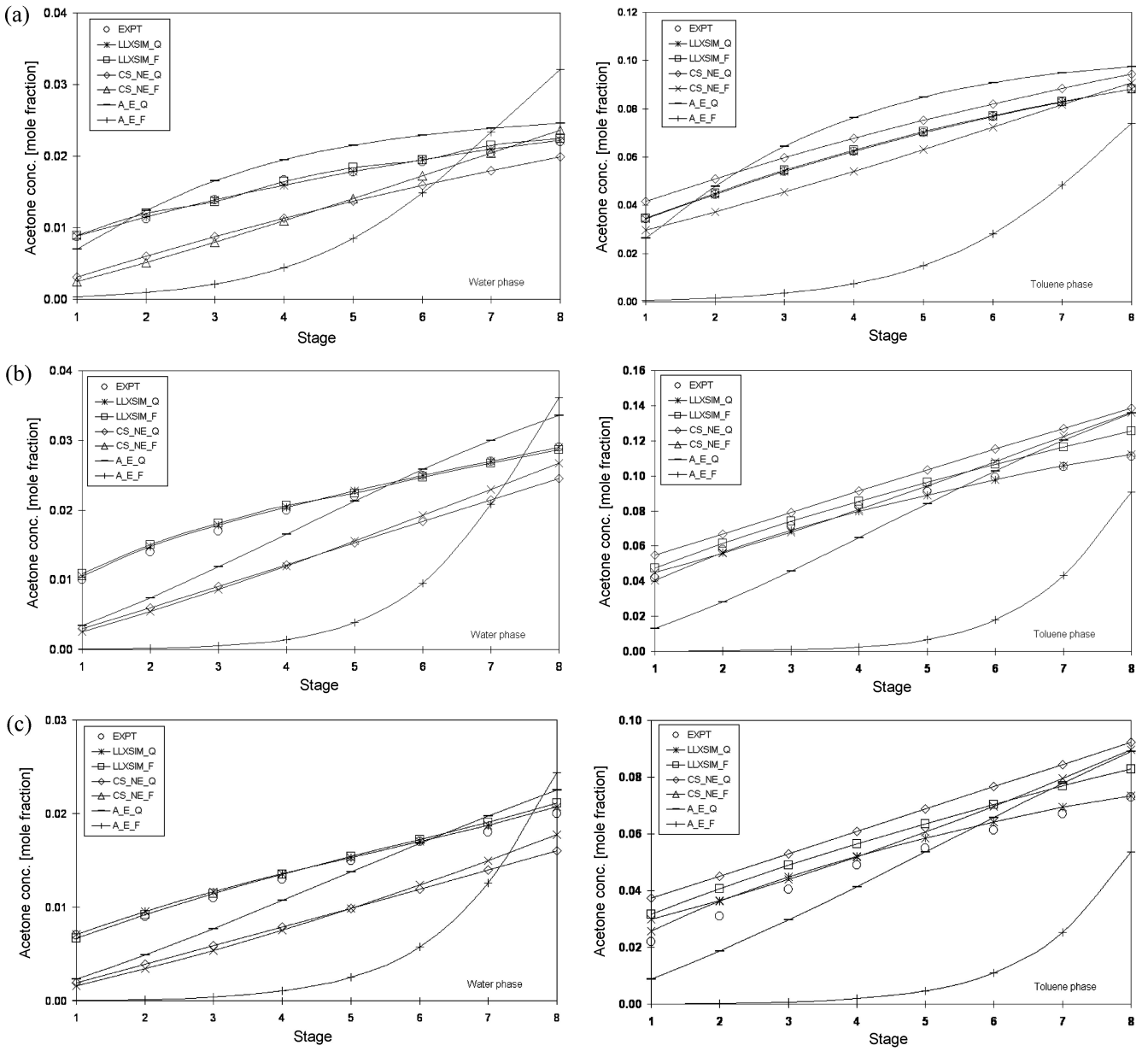

Fig. 3. (a) Acetone concentration profile in Water and Toluene phases (Run # 1). (b) Acetone concentration profile in Water and Toluene phases (Run # 8). (c) Acetone concentration profile in Water and Toluene phases (Run # 10).

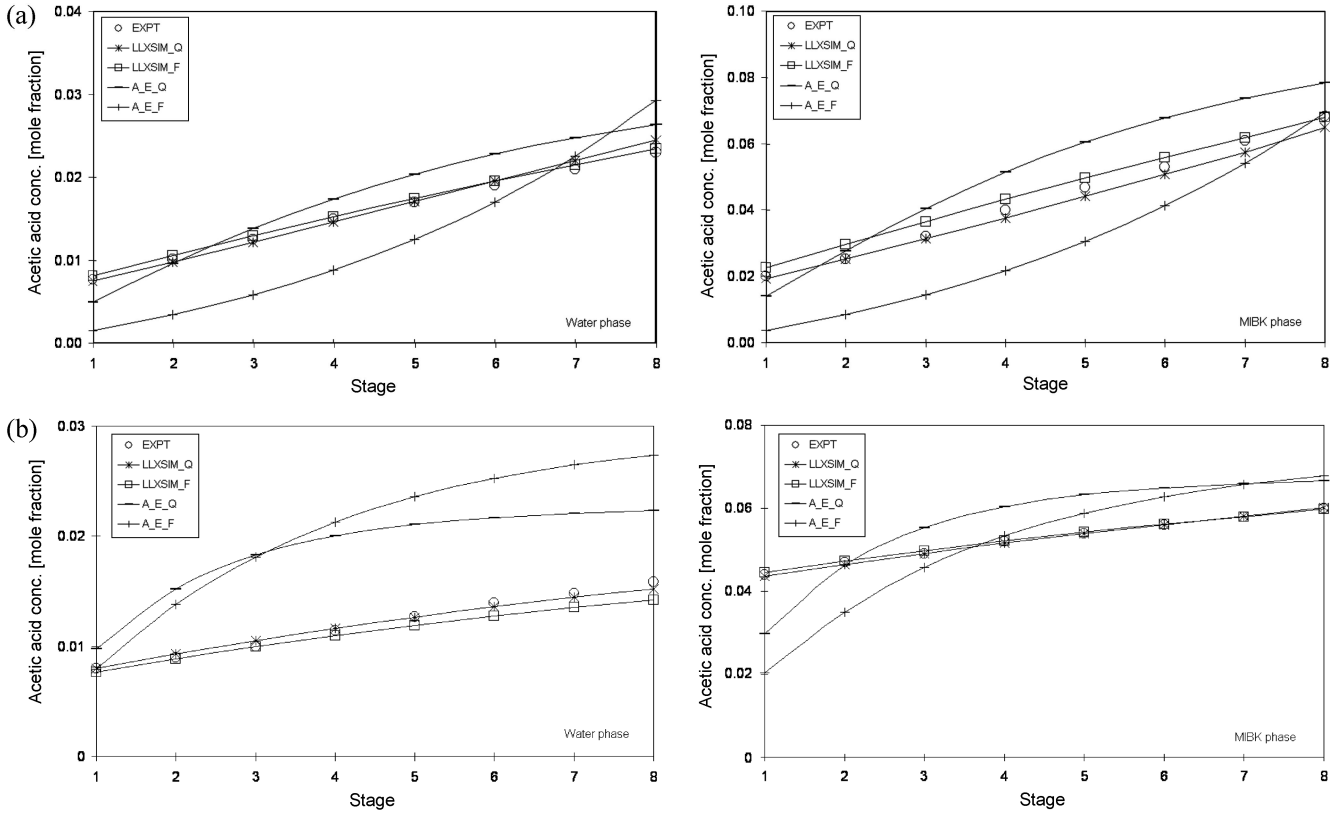

Fig. 4. (a) Acetic acid concentration profile in Water and MIBK phases (Run # 13). (b) Acetic acid concentration profile in Water and MIBK phases (Run # 16).

1986] for infinite dilution diffusivity have been used. On the other hand, in the LLXSIM parallel-parallel mass transfer model [Sanpui and Khanna, 2003] binary mass transfer correlation [Skelland and Conger, 1973], instead of Handlos-Baron, has been used. The MAW system is not available in CHEMSEP simulator; thus MAW simulations were done in ASPENPLUS and LLXSIM.

LLE binary interaction parameters are important in liquid-liquid extraction; we have used two thermodynamic models of liquid-liquid equilibria - UNIFAC and UNIQUAC. UNIQUAC binary interaction parameters are system dependent. In ASPENPLUS, approximate binary parameters (UNIQUAC) are calculated from UNIFAC parameters for the respective systems. Thus, those (UNIQUAC binary parameters) have been borrowed from DECHEMA [Macedo and Rasmussen, 1987] at the temperature of the lab scale experiments and used **as DECHEMA option** in ASPENPLUS. UNIQUAC and UNIFAC parameters for both TAW and MAW systems are reported in Table 3. Simulation runs for the three simulators and the two thermodynamic options can be denoted as follows:

ASPENPLUS	:	A_E_**F**	and	A_E_**Q**
CHEMSEP	:	CS_NE_**F**	and	CS_NE_**Q**
LLXSIM	:	LLXSIM_**F**	and	LLXSIM_**Q**

The **F** and **Q** indicate the use of UNI**F**AC and UNI**Q**UAC. Results are briefly discussed below.

4-1. Composition Profiles

After carrying out all the simulator runs, we plotted the experimental and simulator data points in the same graph. Experimental and simulated Acetone concentration profiles (for the TAW system) in both the Water and Toluene phases for three selected runs are shown in Fig. 3. Similarly, Acetic Acid concentration profiles (for MAW system) in both the MIBK, Water phases were plotted for different concentrations of solute in feed and at solvent to feed ratio Fig. 4. For the ASPENPLUS simulator it has been assumed that the column is 100% efficient. The relative error-squares for all the data points have been calculated. The relative error-square for all the simulation runs with respect to experimental data have been presented in Tables 4 and 5. It has been observed that the experimental data points closely match with LLXSIM non-equilibrium results (with UNIQUAC model) and the sum of the relative error squares is also the minimum. The sum of relative error-square, $RESQ^p$, has been calculated as follows:

$$\text{Relative Error square, } RESQ^p = \sum_{k=1}^{NS}\left[\frac{(\hat{z}_k^p - z_k^{pexpt})}{z_k^{pexpt}}\right]^2 \quad (1)$$

Where $\hat{z}_k^p$=simulated value and z_k^{pexpt}=experimental value of solute concentration in *p*th stage on the *k*th stage.

4-2. Temperature Profiles

ASPENPLUS and CHEMSEP simulators provide only one temperature (i.e., stage temperature) for all the stages. On the other hand, the LLXSIM simulator provides three temperatures - continuous, dispersed phase and the interface temperatures. It was mentioned earlier that we measured the temperatures of both the phases in each stage.

Table 4. RESQ for different simulation options for TAW system

Mole % acetone in feed	*S/F*	LLXSIM_Q	LLXSIM_F	CS_NE_Q	CS_NE_F	A_E_Q	A_E_F
[Acetone in the Water phase]							
Feed temp.=32 °C; Solvent temp.=32 °C							
10	3	0.0033	0.0105	0.9678	1.1721	0.2473	3.5812
10	4	0.0335	0.0960	0.9900	1.1912	0.5846	5.1403
15	3	0.0039	0.1982	0.8894	0.9627	0.2825	NC
15	4	0.0082	0.2910	1.3509	1.4639	0.8670	5.0792
Feed temp.=32 °C; Solvent temp.=40 °C							
10	3	0.0179	0.1822	0.9260	1.1081	0.2531	3.3210
10	4	0.0224	0.2836	1.3506	1.5216	0.7651	5.1242
15	3	0.0051	0.0120	0.9354	0.9937	0.2569	1.7843
15	4	0.0102	0.0198	1.4172	1.4961	0.8196	4.9418
Feed temp.=33 °C; Solvent temp.=50 °C							
10	3	0.0160	0.0530	0.9873	1.1404	0.2126	3.0668
10	4	0.0127	0.0134	1.5157	1.6410	0.8103	4.9968
15	3	0.0029	0.2465	1.0809	1.1100	0.1538	1.4312
15	4	0.0043	0.3690	1.6122	1.6609	0.9270	4.8030
[Acetone in the Toluene phase]							
Feed temp.=32 °C; Solvent temp.=32 °C							
10	3	0.0000	0.0257	0.1034	0.1020	0.2568	4.7598
10	4	0.0222	0.2277	0.8833	0.1457	0.7806	6.0677
15	3	0.0011	0.0137	0.0670	0.0384	0.2659	NC
15	4	0.0210	0.0340	0.1950	0.0955	1.0578	5.9375
Feed temp.=32 °C; Solvent temp.=40 °C							
10	3	0.0000	0.0303	0.1170	0.0729	0.2553	4.5502
10	4	0.0191	0.2164	0.6558	0.1081	0.8063	6.0178
15	3	0.0002	0.0247	0.0917	0.0203	0.2748	2.4244
15	4	0.0060	0.0614	0.2895	0.0978	1.0003	5.8058
Feed temp.=33 °C; Solvent temp.=50 °C							
10	3	0.0002	0.0359	0.1343	0.0447	0.2523	4.2495
10	4	0.0827	0.4412	1.1095	0.2846	0.6934	5.8331
15	3	0.0026	0.0429	0.1336	0.0073	0.3090	1.9812
15	4	0.0010	0.1168	0.4391	0.1481	0.9294	5.6217

**NC Not converged.

The simulated and experimental temperature profiles (for two runs) have been compared for both the TAW and MAW systems and those are shown in Fig. 5. The temperatures in both the phases match closely with the LLXSIM results.

4-3. Hydrodynamic Profiles

Comparing composition and phase temperature profiles between simulators and the experiment is not sufficient. Several hydrodynamic aspects of liquid-liquid extraction need to be considered. There are several hydrodynamics aspects in liquid-liquid extraction. The static hold-up (height of coalesced layer), dynamic hold-up, number of drops [12] in the dispersed phase--these have been calculated in the LLXSIM simulator as follows:

Static hold up: $h_{sk}=h_{\gamma k}+h_{Nk}+h_{ck}$ (2)

Layer thickness to overcome the interfacial tension effect in the dispersed phase,

$$h_{\gamma k}=\frac{0.01\gamma_k(\mu_k^d)^{0.4}(\mu_k^c)^{0.2}}{\Delta\rho_k(d_{Nk})^{1.4}} \quad (3)$$

Layer thickness to overcome the friction in nozzle in the continuous phase,

$$h_{Nk}=\frac{u_{Nk}^2\left[1-\left(\frac{A_p}{A_0}\right)^2\right]\rho_k^d}{2(1-0.71/\log Re_k^d)^2\Delta\rho_k} \quad (4)$$

Layer thickness to overcome the resistance in downspout,

$$h_{ck}=4.5\left[\frac{(u_k^c)^2\rho_k^c}{2\Delta\rho_k}\right] \quad (5)$$

It was mentioned earlier that the heights of the coalesced layer in

Table 5. RESQ for different simulation options for MAW system

[Acetic Acid in the Water phase]					
Mole % acetic acid in feed	*S/F*	LLXSIM_Q	LLXSIM_F	A_E_Q	A_E_F
Feed temp.=30 °C; Solvent temp.=30 °C					
9.3	3	0.0110	0.0088	0.2993	1.6937
Feed temp.=30 °C; Solvent temp.=45 °C					
9.25	3	0.0185	0.0251	0.2535	1.6030
Feed temp.=30 °C; Solvent temp.=45 °C					
9.25	2	0.0261	0.0519	3.2297	4.5793
Feed temp.=33.5 °C; Solvent temp.=50 °C					
7.15	2	0.0072	0.0335	2.9283	4.2312
Feed temp.=33.5 °C; Solvent temp.=50 °C					
7.15	3	0.0138	0.0175	0.1810	1.0502
[Acetic Acid in the MIBK phase]					
Mole % acetic acid in feed	*S/F*	LLXSIM_Q	LLXSIM_F	A_E_Q	A_E_F
Feed temp.=30 °C; Solvent temp.=30 °C					
9.3	3	0.0151	0.0824	0.4770	1.7796
Feed temp.=30 °C; Solvent temp.=45 °C					
9.25	3	0.0282	0.0346	0.4195	1.8182
Feed temp.=30 °C; Solvent temp.=45 °C					
9.25	2	0.0048	0.0061	0.1797	0.5640
Feed temp.=33.5 °C; Solvent temp.=50 °C					
7.15	2	0.0003	0.0005	0.2336	0.4192
Feed temp.=33.5 °C; Solvent temp.=50 °C					
7.15	3	0.0505	0.0165	0.3123	1.1755

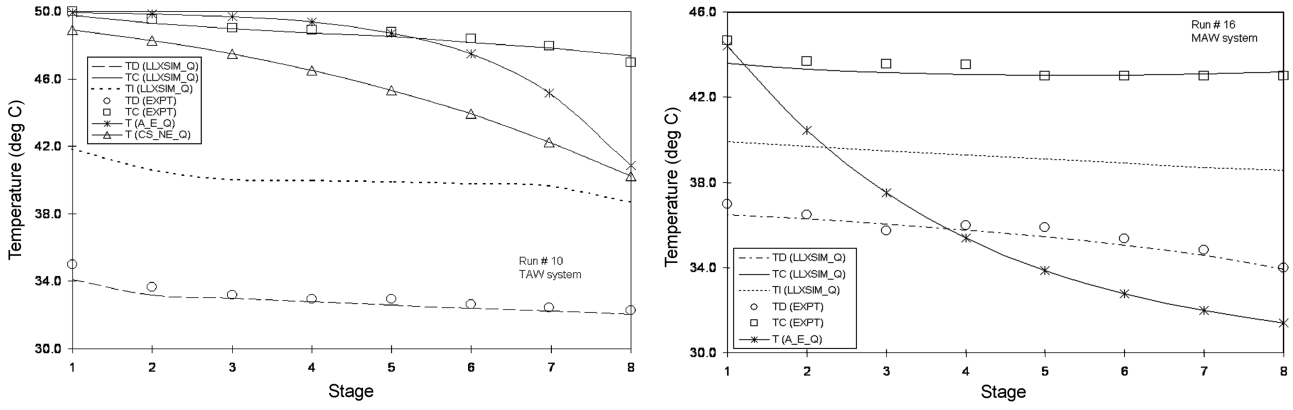

Fig. 5. Temperature profiles for TAW and for MAW.

all the stages were measured for all the experiments. The dynamic hold-up in the stages for the experiments can be calculated as shown, and the numbers of drops (n_{0k}) in the phase have been counted by using photographs as taken at the time of experiments.

Number of drops in the dispersed phase in the *k*th stage,

$$n_{0k} = a_k/(\pi d_{pk}^2/4) \quad (6)$$

The comparative results for the static hold-up and the number of drops in the dispersed phase for the TAW system are shown in the Fig. 6.

4-4. Tuning of Stage Efficiency

Different stage efficiencies have been tried for the ASPENPLUS. In this approach also the experimental and simulator data points have been plotted on the same graph and the sum of the relative error square for all the data points calculated. To show the simulation results ASPENPLUS was run for the three different concentra-

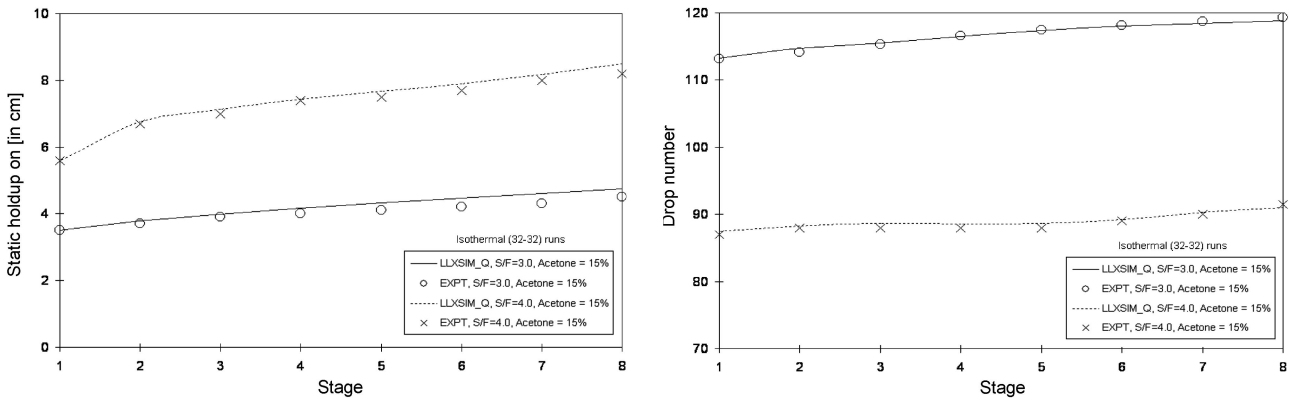

Fig. 6. Hydrodynamic profiles (static holdup and drop number) for TAW system.

Table 6. RESQ for A_E_Q with average stage efficiencies

[Acetone in Water phase]

		Efficiencies						
Mole % acetone in feed	*S/F*	50%	70%	90%	100%	110%	130%	150%
Feed temp.=32 °C; Solvent temp.=32 °C								
10	4	5.449	3.8102	1.4541	0.5846	0.3400	0.6233	0.6529
15	4	5.743	4.3683	2.0448	0.8670	0.2769	0.1212	0.1797
Feed temp.=32 °C; Solvent temp.=34 °C								
10	4	5.5262	3.9847	1.7310	0.7650	0.2588	0.1169	0.1805
15	4	5.7186	4.3401	2.0003	0.8196	0.2376	0.1320	0.2289
Feed temp.=33 °C; Solvent temp.=50 °C								
10	4	5.5228	4.0064	1.7750	0.8104	0.29308	0.1242	0.1911
15	4	5.7270	4.3764	2.1007	0.9269	0.28342	0.0889	0.2213

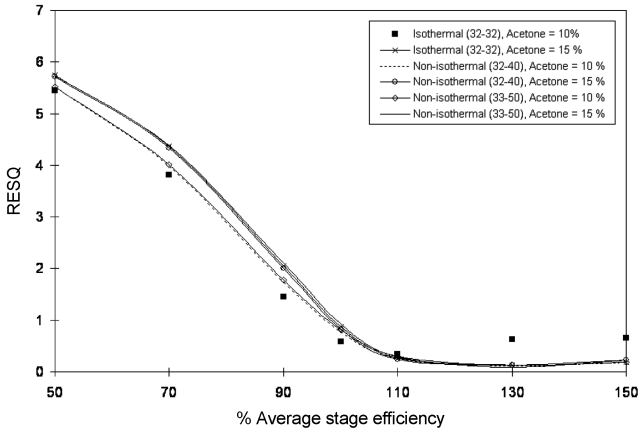

Fig. 7. RESQ with average stage efficiency in ASPENPLUS for TAW system.

tions of Acetone in feed and at solvent to feed ratio 4 : 1. The relative error squares with respect to experimentations are presented in Table 6. The ASPENPLUS simulations for different efficiencies have significant error with respect to experimental data. The sum of relative error square reaches a minimum in the average column efficiency range 90 to 110%. This is shown in Fig. 7. However, this minimum itself is two to ten times higher than that for non-equilibrium options.

CONCLUSION

It has been observed that the experimental results closely match with the rate-based LLXSIM simulator results. The sum of error square analysis (RESQ) shows that deviation between experimental and simulation options is minimum for LLXSIM runs both with UNIFAC and UNIQUAC models. Experimental hydrodynamic features - height of static holdup and number of drops in stage are close to the LLXSIM simulated results. Tuning the average efficiencies for the ASPENPLUS equilibrium model does not result in an acceptable match with the experimental results. The sum of error square analysis for ASPENPLUS efficiency in the range of 50% to 150% still shows errors which are ten times higher in comparison with the LLXSIM non-equilibrium model.

APPENDIX

(Details have been presented by Debjit and Khanna, 2000, *PETCON* 2000, IIT Kharagpur, India and presently in press. *AIChE J.*, 2003)

Component Mass Balance

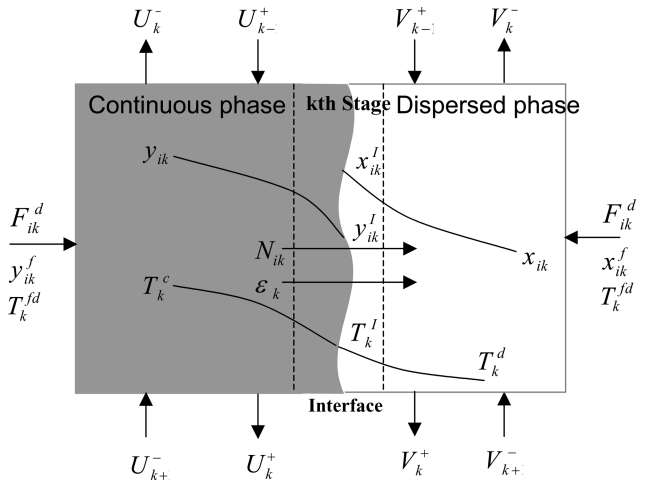

Fig. A.1. Schematic diagram of a non-equilibrium stage with heavy dispersed phase.

Mass balance of *i*th component on kth stage for dispersed phase.

$$V^{+}_{k-1}x_{ik-1}-(V^{+}_{k}+V^{-}_{k})x_{ik}+V^{-}_{k+1}x_{ik+1}+V^{d}_{k}x^{f}_{ik}+N_{ik}=0 \quad (A.1)$$

Mass balance of *i*th component on *k*th stage for continuous phase.

$$U^{+}_{k-1}y_{ik-1}-(U^{+}_{k}+U^{-}_{k})y_{ik}+U^{-}_{k+1}y_{ik+1}+F^{c}_{k}y^{f}_{ik}+N_{ik}=0 \quad (A.2)$$

Phase Equilibrium

Liquid-liquid equilibrium at the inter-phase for *i*th component on *k*th stage.

$$K_{ik}x^{I}_{ik}-y^{I}_{ik}=0 \quad (A.3)$$

Normalization

Normalization equations on the *k*th stage at the interfaces and bulk phases are given below:

$$\sum_{i=1}^{NC}x^{I}_{ik}=1.0 \quad (A.4) \qquad \sum_{i=1}^{NC}y^{I}_{ik}=1.0 \quad (A.5)$$

$$\sum_{i=1}^{NC}x_{ik}=1.0 \quad (A.6) \qquad \sum_{i=1}^{NC}y_{ik}=1.0 \quad (A.7)$$

Energy Conservation

Energy balance on *k*th stage for dispersed phase.

$$V^{+}_{k-1}H^{d}_{k-1}-(V^{+}_{k}+V^{-}_{k})H^{d}_{k}+V^{-}_{k+1}H^{d}_{k+1}+F^{d}_{k}H^{fd}_{k}+\varepsilon^{d}_{k}=0 \quad (A.8)$$

where, $$\varepsilon^{d}_{k}=\sum_{i=1}^{NC}N^{d}_{ik}H^{d}_{ik}+a_{k}h^{d}_{k}(T^{I}_{k}-T^{d}_{k}) \quad (A.9)$$

Energy balance on *k*th stage for continuous phase

$$U^{+}_{k-1}H^{c}_{k-1}-(U^{+}_{k}+U^{-}_{k})H^{c}_{k}+U^{-}_{k+1}H^{c}_{k+1}+F^{c}_{k}H^{fc}_{k}+\varepsilon^{c}_{k}=0 \quad (A.10)$$

where, $$\varepsilon^{c}_{k}=\sum_{i=1}^{NC}N^{c}_{ik}H^{c}_{ik}+a_{k}h^{c}_{k}(T^{c}_{k}-T^{I}_{k}) \quad (A.11)$$

Flow Relationship

Forward flow on *k*th stage for dispersed phase

$$V^{+}_{k}-\left(u^{d}_{k}+\frac{D^{d}_{k}}{\Delta h_{k}}\right)\phi_{k}c^{d}_{k}A_{o}=0 \quad (A.12)$$

Backward flow on *k*th stage for dispersed phase

$$\text{for k=1…NS-1} \quad V^{-}_{k}-\left(\frac{D^{d}_{k-1}}{\Delta h_{k-1}}\right)\phi_{k}c^{d}_{k}A_{o}=0 \quad (A.13)$$

$$\text{for k=NS} \quad V^{-}_{k}=0.0 \quad (A.14)$$

Backward flow on *k*th stage for continuous phase

$$\text{for k=1…NS-1} \quad U^{+}_{k}-\left(\frac{D^{c}_{k}}{\Delta h_{k}}\right)(1-\phi_{k})c^{c}_{k}A_{o}=0 \quad (A.15)$$

$$\text{for k=1} \quad U^{+}_{k}=0.0 \quad (A.16)$$

Forward flow on *k*th stage for continuous phase

$$U^{-}_{k}-\left(u^{c}_{k}+\frac{D^{c}_{k-1}}{\Delta h_{k-1}}\right)(1-\phi_{k})c^{c}_{k}A_{o}=0 \quad (A.17)$$

Mass Transfer Rate

Interface flow balance, based on dispersed phase for *i*th component on *k*th stage.

$$N_{ik}=x_{ik}\sum_{i=1}^{NC}N_{ik}+a_{k}[\kappa]^{d}_{k}(x^{I}_{ik}-x_{ik}) \quad (A.18)$$

Interface flow balance, based on continuous phase for *i*th component on *k*th stage

$$N_{ik}=y_{ik}\sum_{i=1}^{NC}N_{ik}+a_{k}[\kappa]^{c}_{k}(y_{ik}-y^{I}_{ik}) \quad (A.19)$$

Energy Rate

Energy transfer rate or energy balance at the interface on *k*th stage.

$$\sum_{i=1}^{NC}(N^{c}_{ik}H^{c}_{ik})+a_{k}h^{c}_{k}(T^{c}_{k}-T^{I}_{k})-\left\{\sum_{i=1}^{NC}(N^{d}_{ik}H^{d}_{ik})+a_{k}h^{d}_{k}(T^{I}_{k}-T^{d}_{k})\right\}=0 \quad (A.20)$$

NOMENCLATURE

a : interfacial area [m^2]
A : cross sectional area [m^2]
c : molar density [mol/m^3]
d : diameter [m]
D : axial dispersion coefficient [m^2/s]
F : side feed to stage [mol/s]
h : heat transfer coefficient [W/m^2K]
H : partial molar enthalpy [J/mol]
η : height [m]
K : distribution coefficient/equilibrium ratio
n_0 : number of perforation per plate/no of drops
NC : the number of components in the liquid mixture
NS : number of stages
N : inter-phase mass transfer rate [mol/s]
Re : Reynolds number
T : temperature [K]
u : velocity [m/s]
U^{+} : inter-stage backward molar flow rate of continuous phase [mol/s]
U^{-} : inter-stage forward molar flow rate of continuous phase [mol/s]
V^{+} : inter-stage forward molar flow rate of dispersed phase [mol/s]

V^- : inter-stage backward molar flow rate of dispersed phase [mol/s]
x : mole fraction of dispersed phase
y : mole fraction of continuous phase

Greek Letters

ε : inter-phase energy transfer rate [w/m^2 K]
γ : interfacial tension [N/m]
π : 3.14
$\boldsymbol{\kappa}$: binary mass transfer coefficient matrix
ρ : density of liquid [kg/m^3]
$\Delta\rho$: positive difference in density [kg/m^3]
μ : viscosity of liquid [kg/m s]
ϕ : dynamic hold up volume of dispersed phase

Superscripts

c : continuous phase
d : dispersed phase
expt : experimental
I : interface
p : phase

Subscripts

i : component
j : component
k : stage
N : nozzle
0 : column
p : drop, perforation

REFERENCES

AspenPlus Ver 10.0 developed by Aspen Technology, Inc. Cambridge, Massachusetts, USA.

ChemSep Ver 3.71, CACHE Student Edition, developed by Kooijman, H., Haket, A., Taylor, R. (1988).

Chun, B. S., Lee, H. G., Cheon, J. K. and Wilkinson, G., "Mass Transfer in a Countercurrent Spray Column at Supercritical Conditions," *Korean J. Chem. Eng.*, **13**, 234 (1996).

Debjit, S. and Khanna, A., "Rate-Based and Non-Isothermal Aromatic Extraction Column Model," Proc. PETCON 2000, IIT Kharagpur, India, Jul. 1-2, 149.

Handlos, A. E. and Baron, T., "Mass and Heat Transfer from Drops in Liquid-liquid Extraction," *AIChE J.*, **3**, 127 (1957).

Kehat, E. and Ghitis, B., "Simulation of an Extraction Column," *Comp. and Chem. Eng.*, **5**, 171 (1981).

Macedo, E. A. and Rasmussen, P., "Liquid-liquid Equilibrium Data Collection," Supplement 1, Chemistry Data Series, Volume V, Part 4, DECHEMA, **270**, 495 (1987).

Sanpui, D. and Khanna, A., "Selection of Mass Transfer Correlations for Rate Based Liquid-Liquid Model," *Korean J. Chem. Eng.*, **20**, 609 (2003).

Siddiqi, M. A. and Lucas, K., "Correlation for Prediction of Diffusion in Liquids," *Can. J. Chem. Eng.*, **64**, 839 (1986).

Skelland, A. H. P. and Conger, W. L., "Rate Approach to Design of Perforated Plate Extraction Columns," *Ind. Eng. Chem. Proc. Des. & Dev.*, **12**, 448 (1973).

Weidlich, U. and Gmehling, J., "A Modified UNIFAC Model 1. Prediction of Vapor Liquid Equilibria," *Ind. Eng. Chem. Res.*, **26**, 1372 (1987).

Wesselingh, J. A. and Krishana, R., "Mass Transfer," Ellishorwood, Chichester, England (1990).

Zimmermann, A., Joulia, X., Gourdon, G. and Gorak, A., "Maxwell-Stefan Approach in Extraction Design," *The Chem. Engg. J.*, **57**, 229 (1995).